

Topoclimates, refugia, and biotic responses to climate change

David D Ackerly^{1,2*}, Matthew M Kling¹, Matthew L Clark³, Prahlad Papper¹, Meagan F Oldfather⁴, Alan L Flint⁵, and Lorraine E Flint⁵

Plant distributions are strongly influenced by both climate and topography. In an analysis of geographic and topographic distributions for selected tree species in California, we found that tree populations are increasingly restricted to extreme topographic positions as they approach the edge of their geographic ranges, occupying cooler, pole-facing slopes (at the warm and dry edge) and warmer, equator-facing slopes (at the cool and moist edge). At a local scale, species distributions across topographic gradients also correlate with species geographic ranges (species that occupy cooler locations within the landscape have cooler, moister geographic distributions, and vice versa). Model outputs indicated that species found on pole-facing slopes and equator-facing slopes will experience population declines and population increases, respectively, in response to a warmer and drier future. As such, tree species occupying cooler landscape locations, which are viewed as refugia in some contexts, may be most threatened by anthropogenic climate change.

Front Ecol Environ 2020; 18(5): 288–297, doi:10.1002/fee.2204

In the face of rapid climate change, physically heterogeneous landscapes, with different abiotic environments in close proximity, play an important role (Lawler *et al.* 2015), given that they are expected to promote biological diversity in a changing climate for two distinct reasons. First, heterogeneous landscapes produce a diversity of conditions suitable for species with different niche requirements and functional strategies (Kreft and Jetz 2007). The resulting biological diversity serves as a “portfolio” strategy as environmental conditions change, as such variety increases the chances that at least some

of the species will be well suited to future conditions (Figgie 2004). Second, heterogeneous landscapes reduce the distances that species must move to track suitable conditions, effectively reducing the velocity of climate change (Loarie *et al.* 2009; Ackerly *et al.* 2010); this should enhance the persistence of species that are able to find appropriate conditions within reach of their dispersal capacity. This prediction is supported by patterns of endemic diversity (Sandel *et al.* 2011) and local extinction rates observed in the 20th century (Suggitt *et al.* 2018).

In a nutshell:

- Understanding how climate and topography influence plant and animal distributions has taken on a renewed urgency as the planet continues to warm in the 21st century
- Different locations on a landscape, such as pole- and equator-facing slopes, create local microclimates with distinct plant communities
- Species that live in a cool location (eg a north-facing slope, in the northern hemisphere) are often adapted to cooler climates and may be near the edge of their geographic range; this would make them especially vulnerable to a warmer and drier future climate
- Recognizing these patterns will prove important to identify “climate-smart” conservation priorities and strategies

Because they contain a wide range of microclimatic conditions, heterogeneous landscapes are also expected to harbor climate refugia (Ashcroft 2010; Hannah *et al.* 2014; Morelli *et al.* 2017). Although defining climate refugia remains a subject of debate (Keppel *et al.* 2012; Morelli *et al.* 2020), we focus on the landscape scale, and on whether species occupying cool and/or moist locations will be more vulnerable to a warming climate than species in warm and/or dry locations. Cool microsites are often viewed as potential refugia (eg Gollan *et al.* 2014), given that they harbor species adapted to cooler climates, but this notion has also been called into question because these particular species may be the most vulnerable to further warming. At the same time, warm and dry locations within a landscape will become even warmer in the future and will exceed the historical range of variability for the site, and as such species occupying these sites are likely to encounter intolerable conditions in the future. In the context of the papers in this Special Issue, however, we are unable to evaluate whether some sites along this continuum will be buffered and experience less change than others in response to regional climate change (see below).

To evaluate the vulnerability of cool versus warm microsites, we considered the plant community within a specific landscape in relation to the overall geographic and climatic

¹Department of Integrative Biology, University of California–Berkeley, Berkeley, CA *(dackerly@berkeley.edu); ²Department of Environmental Science, Policy, and Management, University of California–Berkeley, Berkeley, CA; ³Department of Geography, Environment, and Planning, Sonoma State University, Rohnert Park, CA; ⁴Department of Ecology and Evolutionary Biology, University of Colorado, Boulder, CO; ⁵US Geological Survey, Sacramento, CA

distributions of the constituent species. The local distribution of a species in relation to topography and microclimates will depend on where the site is located relative to the species' overall geographic and climatic distribution. Natural-history observations often indicate that species tend to shift across topographic and edaphic (soil-related) gradients, when comparing the warm versus cool, or dry versus moist, edges of their distributions (Whittaker and Niering 1965; Holland and Steyn 1975). Boyko (1947) termed these topographical shifts the “geo-ecological law of distribution”, noting that local populations at the dry edge of a plant species range shift toward pole-facing (as opposed to equator-facing) slopes. These locations receive less insolation (the amount of solar radiation received at a given site over time) and the reduced water demand offsets the reduction in precipitation.

As few ecological patterns behave as absolute “laws”, we propose the term “hydroclimatic compensation model” (HCM) as a conceptual framework relating regional climate and locally mediated effects of elevation, topography, soils, and associated factors. With respect to topography, the HCM posits that, at the climatic limits of a species range, populations will be narrowly restricted to cool or warm locations within a landscape (Figure 1). This pattern indicates that where a species is restricted to *cool* locations within a landscape, it is approaching the *warm* edge of its regional climatic niche. As a result, we would expect these populations to be more sensitive to a warming climate (as mentioned above). Although spatial patterns from the HCM match field observations, we are not aware of studies that quantify relationships between topographic distributions and species climatic niches, and that examine how these relationships may affect current understanding of climatic refugia and refugial populations in the face of climate change.

Topography and microclimate

Topography affects plants through the interaction of above- and belowground conditions, coupled with vegetation feedbacks (Moeslund *et al.* 2013). Here, we focus on the effects of solar exposure on pole- versus equator-facing hillsides (henceforth “north-facing” and “south-facing”, from the perspective of the northern hemisphere). Due to planetary geometry, the differences in energy load between north- and south-facing slopes are greatest at the mid-latitudes (Holland and Steyn 1975), so the discussion here is most relevant to mid-latitude, terrestrial vegetation. Assessing ecosystem water balance allows for a better understanding of the integrated effects of topography, soils, and climate (Stephenson 1990; Flint *et al.* 2013), because it reflects seasonal patterns of water availability relative to total energetic demand, which is measured as potential evapotranspiration (PET). Recall that evapotranspiration is the amount of water vapor emitted to the atmosphere by plants (through transpiration) and from

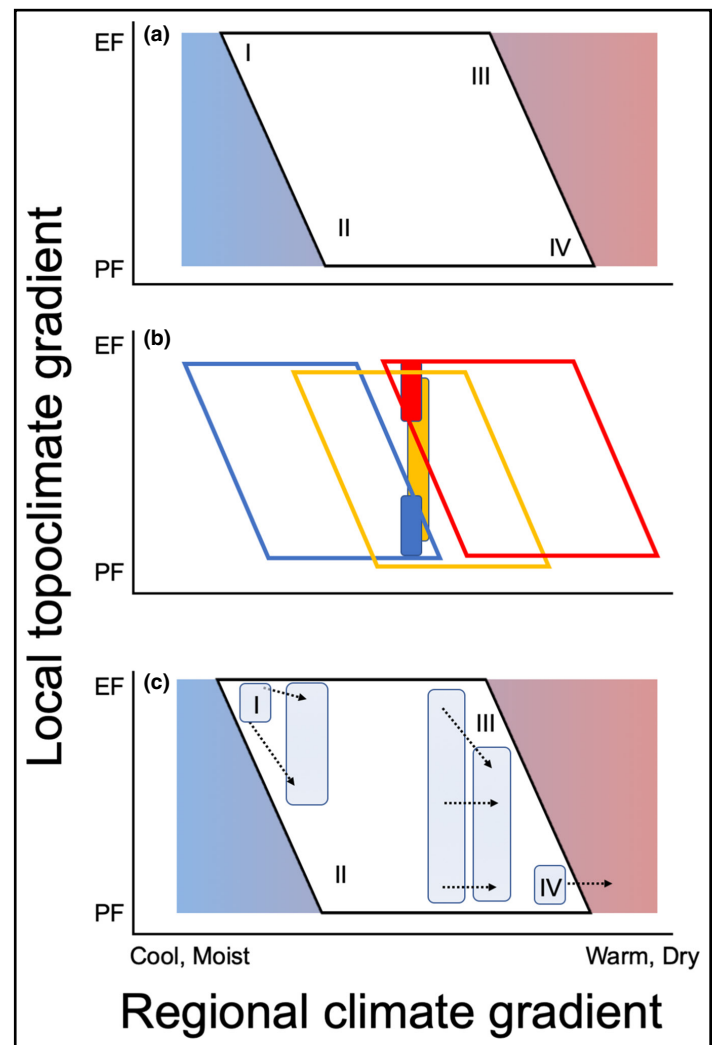


Figure 1. (a) Conceptual diagram of the hydroclimatic compensation model of species distributions along regional climate and local topographic gradients (PF = pole-facing and EF = equator-facing; north- and south-facing, respectively, in the northern hemisphere). I and IV illustrate populations restricted to extreme south or north slopes, respectively, as the species approaches the edge of its climatic distribution; II and III are populations that also occupy north or south slopes, respectively, closer to the middle of the range where the species has a broad topographic distribution. (b) Overlay of three species with contrasting climatic distributions, each represented by a parallelogram of a different color. The colored rectangles show where each species would occur along the local topographic gradient; where those rectangles overlap indicates where the species' local distributions overlap with one another in a single landscape. (c) Conceptual diagram illustrating hypothesized responses to a warming or drying climate. Rectangles indicate where populations would occur under current and future climates, following the trajectory of the arrows. Populations restricted to south-facing slopes (I) are expected to have increasing suitability, which would promote expansion across the landscape. At warmer locations (III), the species range would be expected to contract across the topographic gradient. Populations restricted to cool, north-facing slopes (IV) are threatened with extirpation as they occupy the warm edge of the species range.

soils (through evaporation). While PET describes the amount of water that would be emitted if water availability was unlimited, actual evapotranspiration (AET) depends

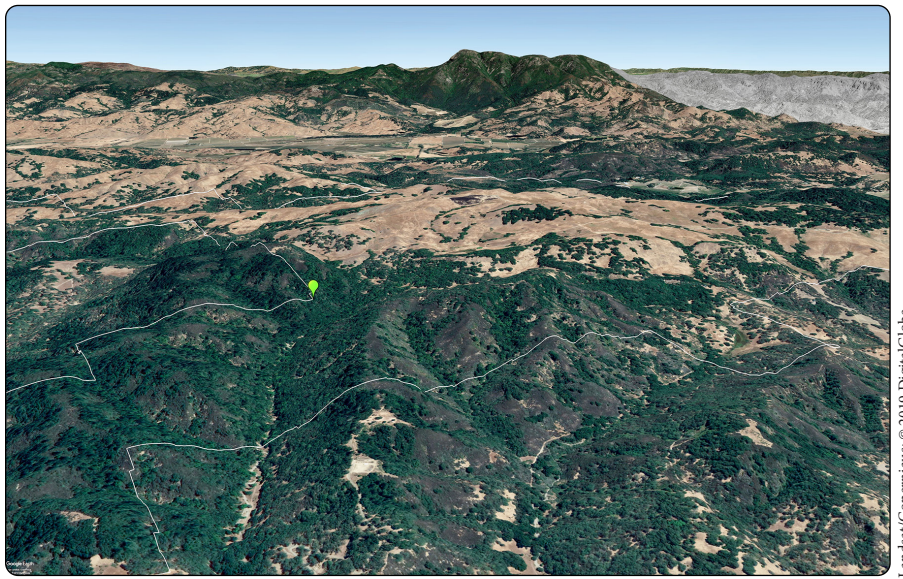


Figure 2. Google Earth image of the Pepperwood Preserve landscape, viewed from the southwest, with Mt Saint Helena in the background, showing the rugged topography and contrasting vegetation on north- versus south-facing slopes. The white line shows the property boundary. The green corner marker provides a reference point shown on the maps in Figure 3, b and d.

on the moisture that is available in the environment and, as such, is usually less than PET; AET therefore reflects how seasonal shifts in energy (ie temperature) versus water act as limits to primary productivity. Conversely, climatic water deficit (CWD) is calculated by subtracting AET from PET, capturing seasonally integrated, excess energy loading relative to water availability. CWD is a particularly relevant measure in a Mediterranean-type climate, as it captures regional and local variation in the intensity of the summer dry season, as well as interannual climatic variability. All things being equal, CWD is higher (1) on south-facing slopes due to higher insolation, (2) on soils with lower moisture-holding capacity (shallower or finer textured soils with lower permeability), and (3) in areas with higher summer temperatures and/or lower rainfall. CWD is a strong predictor of spatial patterns in vegetation (Ackerly *et al.* 2015), responses to long-term climate change (McIntyre *et al.* 2015), and impacts of drought (Das *et al.* 2013; Anderegg *et al.* 2015; Flint *et al.* 2018), and can also be used to assess species distributions and the potential vulnerability of vegetation to future climate change (Franklin *et al.* 2013; McCullough *et al.* 2016; Thorne *et al.* 2017).

Objectives

In this study, we first tested the hydroclimatic compensation hypothesis that species will primarily occur on north-facing slopes at the warm and dry end of their range, and on south-facing slopes toward the cool and/or moist edge of their range. Next, we tested the corollary of this pattern at a local scale, asking whether the topographic distributions

of species within a landscape are correlated with species geographic ranges and climatic niches. Specifically, we predicted that within a single community, the species occupying cooler and wetter microsites (ie north-facing slopes and valley bottoms) are those occupying cooler and wetter locations across their entire geographic ranges. Finally, we used species distribution models coupled with a factorial combination of changing climate conditions to test whether the local topographic distribution of a species is correlated with its predicted response to increasing CWD in a warming climate.

Methods

Note: results that appear within this section represent, or justify the inclusion of, selected inputs to models and analyses.

Site and species

The focal site for this research was Pepperwood Preserve, a protected area in the Coast Ranges of northern California (38.57°N, -122.68°W, Sonoma County). Vegetation at Pepperwood consists of a mosaic of grasslands, shrublands, deciduous oak (*Quercus* spp) woodlands, and mixed hardwood/evergreen forests (Figure 2; Oldfather *et al.* 2016). We focused on 12 tree species that comprise the canopy-dominant, woody vegetation, plus *Adenostoma fasciculatum*, the dominant shrub of evergreen chaparral shrublands (Table 1; Figure 3a).

Regional distributions, climatic niche, and slope position

Species distributions of trees in the western US were obtained from the US Forest Service's Forest Inventory and Analysis (FIA) program (Burrill *et al.* 2018; see WebFigure 1). Data on the distribution of *A fasciculatum* were obtained from herbarium specimens in the Consortium of California Herbaria (CCH; Baldwin *et al.* 2017). For regional climate analyses, we used the CHELSA 1-km interpolated climate dataset (Karger *et al.* 2017), with climatic averages for 1979–2013 covering the western US. Using monthly values for temperature and rainfall, we calculated PET, AET, and CWD (Figure 3c), as well as T_{\min} , which represented the minimum temperature of the coldest month.

For each species, we extracted climatic values for each location in the FIA or CCH dataset. Spatial coordinates of FIA locations are “fuzzed” (intentionally adjusted to ensure that sites remain undisturbed), with locations typically within 1–2 km of the actual site; at the scale of our analysis we assumed that this procedure introduced some random error but no systematic bias in climatic distributions. FIA plot data include

Table 1. Study species

Scientific name (abbreviation)	Common name	Functional group	Landscape abundance	Color*
<i>Adenostoma fasciculatum</i> (Af)	Chamise (= shrubland)	ESS	12.7	red
<i>Acer macrophyllum</i> (Am)	Bigleaf maple	DBT	2.0	black
<i>Aesculus californica</i> (Ac)	California buckeye	DBT	0.5	black
<i>Arbutus menziesii</i> (Az)	Madrone	EBT	11.7	orange
<i>Notholithocarpus densiflorus</i> (Nd)	Tanoak	EBT	1.6	black
<i>Pseudotsuga menziesii</i> (Pm)	Douglas fir	ENT	22.9	dark green
<i>Quercus agrifolia</i> (Qa)	Coast live oak	EBT	17.3	brown
<i>Quercus douglasii</i> (Qd)	Blue oak	DBT	2.4	black
<i>Quercus garryana</i> (Qg)	Oregon oak	DBT	14.9	light green
<i>Quercus kelloggii</i> (Qk)	Black oak	DBT	2.5	black
<i>Quercus lobata</i> (Ql)	Valley oak	DBT	4.5	cyan
<i>Sequoia sempervirens</i> (Ss)	Redwood	ENT	0.9	black
<i>Umbellularia californica</i> (Uc)	California bay	EBT	6.1	yellow

Notes: functional groups: ESS = evergreen sclerophyll shrub; DBT = deciduous broadleaf tree; EBT = evergreen broadleaf tree; ENT = evergreen needleleaf tree. Landscape abundance shows proportion of all woodland and shrubland area occupied by each species (from the hyperspectral canopy map in Figure 3b), excluding herbaceous and non-native vegetation. *Colors correspond to palettes in Figures 3b, 5, and 6 (less common species all shown in black); species abbreviations appear in Figures 5 and 6, as well as in WebTable 1.

measurements of slope and aspect taken onsite (unaffected by “fuzzing”). South-facing exposure (“southness”) was measured as $-\cos(\text{aspect}) \times \sin(\text{slope})$, which ranges from -1 to 1 for vertical north-facing and south-facing slopes, respectively, and 0 for a flat site. We used southness so that higher values for topography as well as CWD represent warmer and/or drier conditions. Although McCune and Keon (2002) provided numerical formulas for calculating topographic heat load – based on slope, aspect, latitude, and an adjustment for the increased heat load on southwest slopes due to higher afternoon temperatures – we preferred to use the simpler southness measure described above, pending future research to determine the optimal aspect adjustment for different landscapes.

We used these climatic, topographic, and distributional data to test the HCM for the 12 focal tree species at both the dry and wet edges of their CWD range, for a total of 24 tests. To isolate the pattern near the niche edge, we used the subset of all FIA plots in the western US that had CWD values between the 90th and 100th percentiles (or 0th and 10th percentiles for wet edge tests) of all plots occupied by the focal species; various percentiles ranging from 50th to 95th were tested and yielded similar results.

For each of the 24 tests, we used logistic regression to predict species occupancy as a function of microsite southness and landscape mean CWD. At the hot and dry (high-CWD) edge of a species range, we expect CWD and southness to have negative effects on occupancy, as species will not be able to tolerate more extreme conditions (and vice versa at low-CWD edges). Our choices to analyze these patterns using logistic regression, a 90th percentile cutoff, and filtering out extreme slopes were based on extensive niche simulations, as described in WebPanel 1.

To obtain measures of the climatic niche of each species, we evaluated univariate generalized additive models (GAM) with binomial link functions, in which climate data at observation locations were combined with a random sample of 10,000 background points selected from an expanded convex hull around the species range (see Guisan *et al.* 2002; Barve *et al.* 2011). Potential spatial autocorrelation (SA) in predictor variables and distribution data was not included in the models. SA strongly exaggerates statistical significance (Segurado *et al.* 2006), which was not a focus of our modeling, and impacts on parameter estimation and uncertainty are observed under some conditions, depending on scale, but not others (Hawkins *et al.* 2007; Paciorek 2010). For CWD, AET, and T_{\min} , the niche optimum for each species was calculated as the climate value at the maximum predicted probability across the regional gradient, and the niche mean was calculated as the weighted mean of climate values, weighted by predicted probabilities.

Pepperwood topoclimate, species distributions, and topographic niche

Across Pepperwood and adjacent landscapes, topography and topoclimate (climatic variation due to slope, aspect, etc) were evaluated using a 10-m resolution digital elevation model. Southness was calculated for each pixel using the formula described above, with values ranging from -0.73 to 0.70 . The topographic wetness index (TWI) was calculated following the approach described in Beven and Kirkby (1979), with values ranging from 1.9 to 22.8 (higher values indicate valley bottoms).

A 10-m resolution version of the Basin Characterization Model was developed for the Pepperwood landscape. The

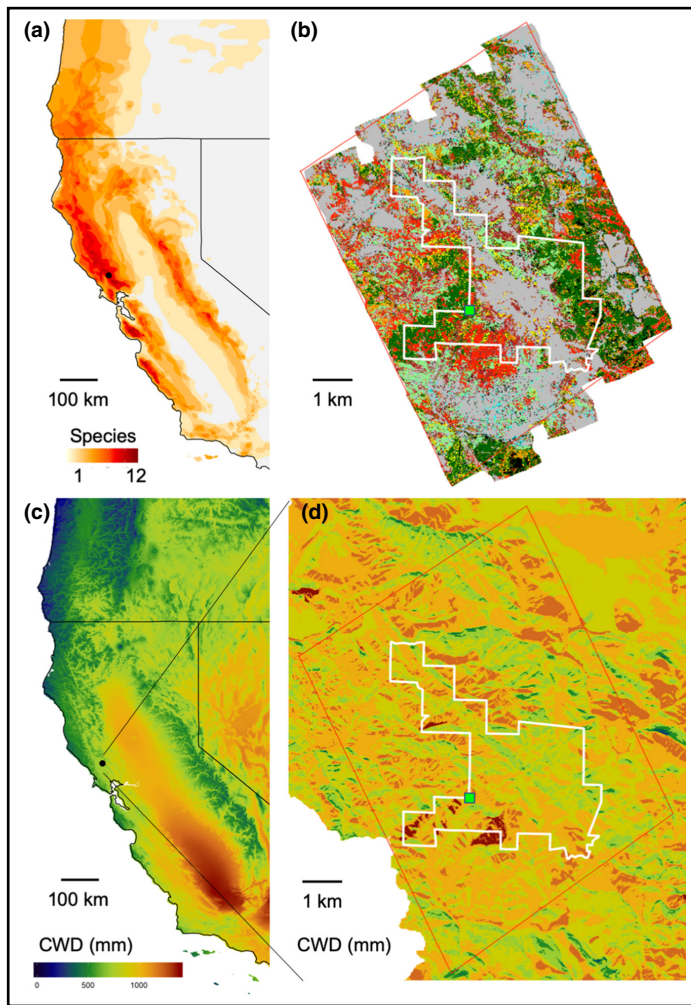


Figure 3. (a) Heat map of species diversity for the 12 focal tree species (Little 1971; see individual species maps in WebFigure 1). Location of the Pepperwood Preserve is indicated by the black circle. Color gradation from light to dark red denotes diversity range from 1 to 12 species. (b) Species distribution map across Pepperwood landscape from the classification of hyperspectral remote-sensing imagery: dark green = Douglas fir (*Pseudotsuga menziesii*); red = shrubland; brown = coast live oak (*Quercus agrifolia*); light green = Oregon oak (*Quercus garryana*); orange = madrone (*Arbutus menziesii*); yellow = California bay (*Umbellularia californica*); cyan = valley oak (*Quercus lobata*); black = other species (see Table 1); gray = grasslands. White outline depicts the Pepperwood Preserve boundary, and the green marker shows the corner point indicated in Figure 2, for reference. (c) Climatic water deficit (CWD, mm) map for California and adjacent regions. Color gradation from blue to red denotes increasing CWD values. (d) CWD map for the Pepperwood landscape (color gradation same as in [c]).

BCM uses regional temperature and precipitation data down-scaled to fine spatial scales (Flint and Flint 2012), soil moisture storage based on mapped soils and their properties, run-off calibrations from local stream gauges, and energy balance based on topographic exposure and cloudiness to calculate monthly and annual AET, PET, and CWD (Figure 3d; Flint et al. 2013). As the climatic influence on CWD is mostly constant across a local landscape, landscape-scale variation in CWD is primarily driven by exposure (slope and aspect) and

soils. In this case, the correlation between southness and CWD was $R = 0.87$, illustrating the primary control by exposure.

We obtained a canopy map of woody species distributions across the Pepperwood landscape based on high-resolution imaging spectroscopy (hyperspectral) remote sensing covering 5845 ha at 2-m pixel resolution (Figure 3b), with tree species mapped using a hierarchical support vector machine (SVM) classifier (Clark et al. 2018; WebPanel 1). Based on field surveys, overall accuracy for the 12 focal tree species was 85.5% at both pixel and crown levels. Shrubland was not differentiated into different types. The majority of shrublands at Pepperwood are composed of mixed stands of chamise (*A fasciculatum*), manzanita (*Arctostaphylos manzanita*), and other chaparral species. For the comparisons below, we used the regional distribution of *A fasciculatum*, which represents the broader California distribution of chaparral, recognizing that the shrublands at Pepperwood contain other species as well.

The canopy map was aggregated to 10-m pixels, calculating the proportion of each pixel occupied by each species, and aligned with topoclimate layers. We calculated topo-climatic niches using three different variables: southness, CWD, and TWI. Following the same method as the regional modeling, we fit a univariate GAM for each species, using topo-climate as a predictor variable and percent occupancy as the dependent variable, with a binomial link function. We then recorded the environmental value at the maximum predicted probability from the model as a measure of optimum topo-climatic niche, and the weighted mean value, weighted by predicted probabilities, as a measure of the niche mean. As for regional models, we did not account for SA at the landscape scale, and we recommend future studies consider this in greater detail. We tested our second hypothesis, concerning the local community predictions of the HCM, by testing for positive correlations between regional (based on FIA and CCH data) and topo-climate (based on the hyperspectral canopy map) niche metrics.

Species distribution models and future projections

Climate-based species distribution models (SDMs) were fit for the focal species using the FIA or CCH distributional data. The three climate variables that were chosen – CWD, AET, and T_{\min} – exhibit very low correlations across the western US, enhancing their performance in model fitting. SDMs were fit with GAMs, using the same presence and background data point selection as described above. Deviance explained by the GAMs ranged from 0.41 for Douglas fir (*Pseudotsuga menziesii*) to 0.85 for coast redwood (*Sequoia sempervirens*), indicating modest to good fits overall.

Projections for historical and future climatic suitability were calculated at the 1-km scale for a 56-km² polygon containing the hyperspectral canopy map. To systematically explore the effects of varying the three climate variables

(CWD, AET, and T_{\min}) used in the model, we constructed four climate-change increments for each variable representing the approximate range of changes projected by late-century climate models in this region (Ackerly *et al.* 2015). For CWD, all future scenarios have increased CWD values, and therefore we used increments of +0 mm (historical), +40 mm, +80 mm, and +120 mm. For AET, scenarios with lower rainfall have reduced AET, while scenarios with higher rainfall have increased AET; therefore, we used increments of -25 mm, +0 mm (historical), +25 mm, and +50 mm. Finally, for T_{\min} , all scenarios exhibit increased temperatures, and therefore we used +0°C (historical), +1°C, +2°C, and +3°C. Sixty-four factorial combinations were constructed using all combinations of these increments. Probabilities for each species were projected for each of the 64 scenarios, and the average across the Pepperwood landscape was calculated for each species and scenario. Linear regression was then used to evaluate the changes in suitability across the domain in relation to changes in the three climate factors. Sensitivities (changes in mean suitability) were calculated for each focal species in the Pepperwood region only, in order to link the results to the species local topographic distributions (Hypothesis 3). As noted above, we assumed that the amount of change will be the same for all locations across the landscape, and that locations will differ only in their initial topoclimate conditions. At present, however, we lack sufficient data to project whether some sites will be buffered and experience less change than others, information that is critical to the broader discussion of potential refugia (Morelli *et al.* 2020).

Results

Hypothesis 1

Across the wet and dry edges of the 12 tree species distributions, 23 of 24 independent tests exhibited the predicted sign of the effect of CWD and southness on the two edges of the distribution (WebTable 1). The logistic regression coefficients can be visualized as a set of parallel contour lines, one of which we plotted for each test (Figure 4). All tests found declining occupancy in landscapes with more extreme (low or high) CWD values, confirming that the dataset encompasses species CWD niche limits, and all were significant except for California buckeye (*Aesculus californica*) at high CWD. All but one of the 24 tests found the predicted negative slope of occupancy contours describing the compensation between the regional CWD gradient and the local southness gradient (18 of 24 were significant at $P < 0.05$; Figure 4; WebTable 1).

Hypothesis 2

The 13 species studied here (12 tree species plus the shrub *A fasciculatum*) had widely varying biogeographic distributions (Figure 3a; WebFigure 1) that overlapped at Pepperwood, which sits at the ecotone between central and

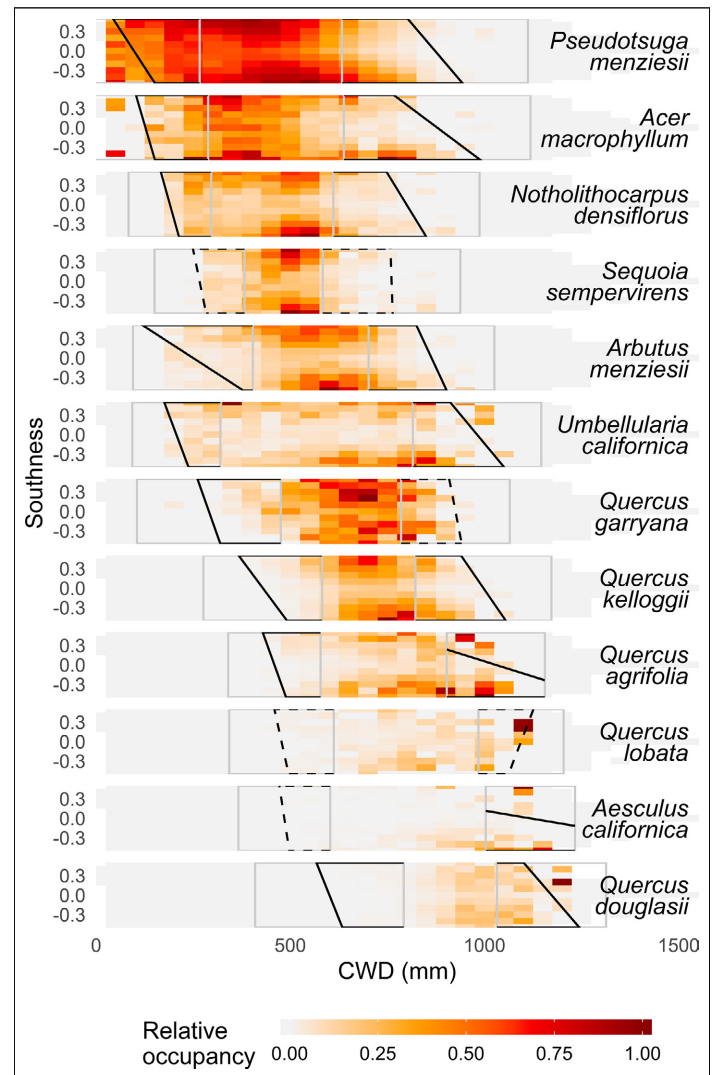


Figure 4. Distributions of tree species from Forest Inventory and Analysis data in relation to regional CWD and topographic position. Diagonal lines represent contour lines of occupancy as a function of CWD and southness, illustrating the shift toward south-facing slopes at low CWD and north-facing slopes at high CWD (see Methods); these contours are parallel for a given model, and the one that passes through the center of the rectangular modeling domain is shown ($P \leq 0.05$ for solid lines); gray boxes indicate lower and upper 10th percentile.

northern coastal California floristic zones. Mean regional CWD, averaged across species distributions, ranged from 334–916 mm for the 13 species. Regional CWD optimum and mean values were very similar across species ($R = 0.94$), and we focused on the mean for further analyses.

Within the Pepperwood landscape, optimum CWD ranged from 343–1385 mm and mean CWD ranged from 806–983 mm, and the two were highly correlated ($R = 0.89$). The wide range for the optima encompasses the entire range of CWD values in the local study domain, as five species had peak predicted probability at the minimum value, and one species at the maximum value (results not shown). The mean values have a narrower range, as most species were

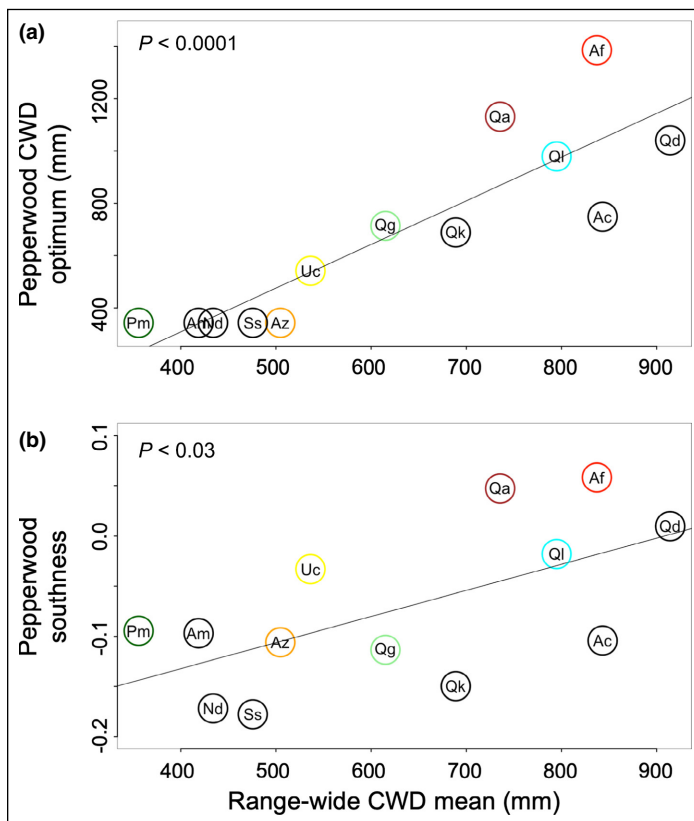


Figure 5. Scatterplots of species distributions on topographic gradients at Pepperwood (local) in relation to range-wide CWD mean. (a) Optimal CWD from the generalized additive model of Pepperwood distributions. (b) Mean southness averaged over all occupied locations. P values are for slope of the linear regressions. See Table 1 for species abbreviations. Colors match those described in Figure 3b.

fairly widely distributed across the landscape but had distinct tendencies to prefer south- versus north-facing slopes. Local mean CWD was also strongly correlated with the mean southness values calculated for each species across occupied sites ($R = 0.98$).

Range-wide mean CWD was significantly correlated with local mean CWD ($R = 0.72$, $P = 0.005$), local optimum CWD ($R = 0.88$, $P \leq 0.001$; Figure 5a), and local mean southness ($R = 0.62$, $P \leq 0.05$; Figure 5b), supporting our predictions for Hypothesis 2 that regional climatic distributions are correlated with local topographic distributions.

Hypothesis 3

Suitability at Pepperwood, extracted from the regional SDM, ranged from 0.28–0.93 across the 13 species. These values ranged from 28–96% of the maximum values across the species entire ranges, demonstrating that for some species Pepperwood was near their optimum climatic conditions while for others it was much farther away.

Across the hypothetical future climate conditions examined here, changes in suitability ranged from -0.89 to $+0.32$, and 87% of all changes were negative. Responses to the three

factors were not significantly correlated with one another. Species responses to increasing CWD were significantly and positively associated with their regional and local topographic niche means, supporting our predictions for Hypothesis 3 (Figure 6). Species whose geographic ranges or local topographic niches occupied higher CWD values (warmer/drier) had more positive responses, while those occupying lower CWD positions (cooler/moister) had more negative responses. Responses to AET and T_{\min} were not associated with regional or topographic CWD niche position (results not shown).

Discussion

This study supports three general conclusions related to climatic refugia and the potential sensitivity of species within a local landscape to anthropogenic climate change. At a regional scale, we find support for the HCM (ie Boyko's "geo-ecological law"), in that within species, populations tend to occupy cool, pole-facing slopes in hot/dry regions and shift to warmer, equator-facing slopes in cool/moist regions (Figures 1 and 4). This pattern is familiar to many field naturalists, and the FIA surveys provide exceptional quantitative data for analysis across multiple species. The example presented here illustrates hydroclimatic compensation driven by topography; other examples that would fit into an expanded framework include shifts to higher elevations at lower latitudes and shifts to deeper soils with reduced precipitation (Stephenson and Das 2011).

As a corollary of this pattern, the distributions of species within a local landscape reflect the position of the site relative to the geographic range of each species. In other words, tree species on cool, pole-facing slopes are those that have cooler geographic distributions overall, whereas species on warm, equator-facing slopes are those that have warmer distributions (Figure 1b). It follows from these patterns, though it may seem somewhat counterintuitive at first, that species in cooler locations within a local landscape are approaching the warm edge of their range at a biogeographic scale (Figure 1a).

On the basis of these observations and our conceptual model, we predicted that species occupying cooler sites within a landscape are projected to decline in response to warmer/drier future climates (ie climatic suitability declines in the locations they currently occupy). We found support for this pattern based on responses to factorial combinations of future climate scenarios. When subjected to future increases in CWD at both regional and landscape scales, species occupying locations with higher deficits (at warm/dry sites) responded positively, while species occupying locations with lower deficits (at cool/moist sites) responded negatively. In contrast, sensitivities to AET and T_{\min} were not associated with landscape-scale distributions; moreover, we also found no relationship between species' geographic distributions on T_{\min} gradients and species' local distributions in relation to cold air pooling (results not shown). This opens an interesting avenue for further research,

focusing on why correspondence across scales may be stronger on some environmental gradients than others.

Our results suggest that tree community composition will shift toward more warm and dry-adapted species, a phenomenon known as thermophilization, which has already been observed in plant communities around the world (De Frenne *et al.* 2013; Duque *et al.* 2015). Building on the HCM, species located on warmer and drier ends of the landscape gradient would be expected to expand toward cooler locations (Figure 1c), replacing species that are declining. Such changes are more likely to occur in landscapes with fine-grained topography (ie many valleys and ridges in a small area), because warm and cool sites are closer together, allowing seeds to disperse more readily across the topoclimate gradient (Engler *et al.* 2009). As a result, these landscapes may experience more rapid biotic responses to climate change at a local scale due to the close proximity of species with varying climatic tolerances. Conversely, hot and dry locations within a landscape may experience lower propagule pressure from newly arriving species, as there are no local populations to serve as source areas for taxa adapted to a hotter climate (Ackerly 2003). If no new species arrive from outside the local area, the local declines of species in cool sites and expansion of hot- and dry-adapted species across the gradient will lead to biotic homogenization and a net loss of diversity.

Looking ahead, these analyses suggest several critical avenues for future research. The first is further study of abiotic buffering or decoupling, to understand whether some microclimates will change more or less than others, relative to regional climatic drivers (Dobrowski 2011). Second is the interaction of abiotic and biotic factors as mechanisms of community change, including the role of competitive interactions among plant species and plant–animal relationships including herbivory, pollination, and dispersal (Ettinger and HilleRisLambers 2013). In particular, rapid environmental change may outpace species dispersal capacities, and therefore local changes will unfold among existing community members even if they are not well suited to the changing conditions. Lastly, tree mortality from ecological disturbances such as fire and drought may provide important regeneration opportunities for other species and may represent critical episodes of biotic change (Millar and Stephenson 2015; Krawchuck *et al.* 2020). Historical baselines and long-term studies of community dynamics will be essential for detecting change in the coming century, understanding the roles of these interacting factors, and determining whether climate refugia play an important role in supporting biodiversity as climate continues to change.

Acknowledgements

Publication of this Special Issue was funded by the US Department of the Interior National, Northeast, and Northwest Climate Adaptation Science Centers. We thank Pepperwood Preserve staff for collaboration and logistical

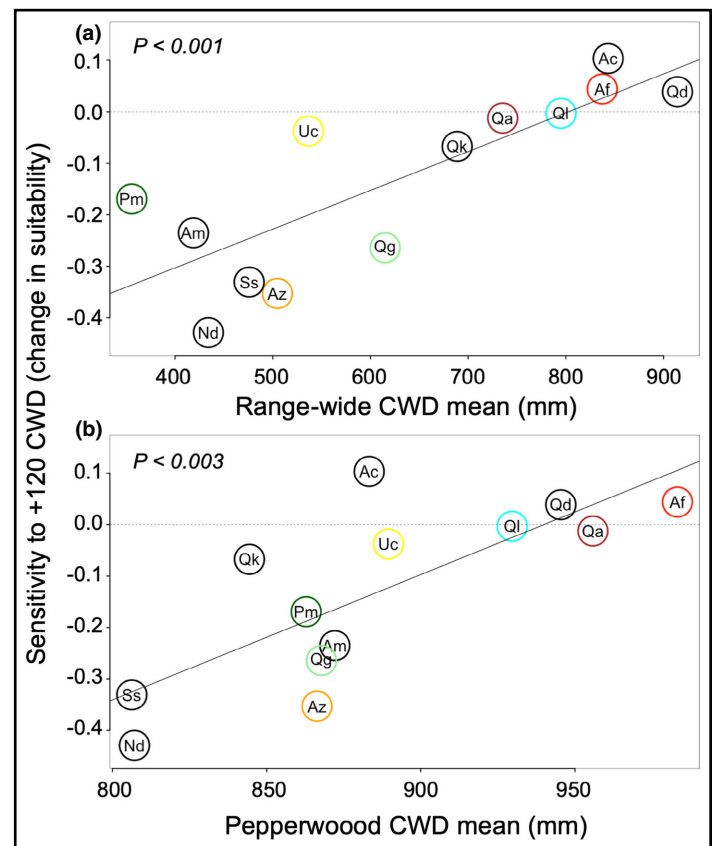


Figure 6. Sensitivity of each species measured as an increase in suitability in response to a 120-mm increase in CWD (holding other factors constant), in relation to (a) regional or (b) local topographic CWD niche. P values are for slope of the linear regressions. See Table 1 for species abbreviations. Colors match those described in Figure 3b.

support of field work. MLC's involvement in this research was supported by the National Aeronautics and Space Administration's (NASA's) HypsIRI Preparatory Airborne Activities and Associated Science Research grant NNX12AP09G. We thank the AVIRIS-NG team at NASA's Jet Propulsion Lab for acquiring imagery and providing atmospheric corrections. MMK's contributions were supported by a US National Science Foundation (NSF) predoctoral research fellowship. This project was supported by NSF grant 1754475.

References

- Ackerly DD. 2003. Community assembly, niche conservatism and adaptive evolution in changing environments. *Int J Plant Sci* **164**: S165–84.
- Ackerly DD, Cornwell WK, Weiss SB, *et al.* 2015. A geographic mosaic of climate change impacts on terrestrial vegetation: which areas are most at risk? *PLoS ONE* **10**: e0130629.
- Ackerly DD, Loarie SR, Cornwell WK, *et al.* 2010. The geography of climate change: implications for conservation biogeography. *Divers Distrib* **16**: 476–87.

- Anderegg WRL, Flint A, Huang C, *et al.* 2015. Tree mortality predicted from drought-induced vascular damage. *Nat Geosci* **8**: 367–71.
- Ashcroft MB. 2010. Identifying refugia from climate change. *J Biogeogr* **37**: 1407–13.
- Baldwin BG, Thornhill AH, Freyman WA, *et al.* 2017. Species richness and endemism in the native flora of California. *Am J Bot* **104**: 487–501.
- Barve N, Barve V, Jiménez-Valverde A, *et al.* 2011. The crucial role of the accessible area in ecological niche modeling and species distribution modeling. *Ecol Model* **222**: 1810–19.
- Beven KJ and Kirkby MJ. 1979. A physically based, variable contributing area model of basin hydrology. *Hydrol Sci B* **24**: 43–69.
- Boyko H. 1947. On the role of plants as quantitative climate indicators and the geo-ecological law of distribution. *J Ecol* **35**: 138–57.
- Burrill EA, Wilson AM, Turner JA, *et al.* 2018. The Forest Inventory and Analysis Database: database description and user guide version 8.0 for Phase 2. Washington, DC: US Department of Agriculture, Forest Service.
- Clark ML, Buck-Diaz J, and Evens J. 2018. Mapping of forest alliances with simulated multi-seasonal hyperspectral satellite imagery. *Remote Sens Environ* **210**: 490–507.
- Das AJ, Stephenson NL, Flint A, *et al.* 2013. Climatic correlates of tree mortality in water- and energy-limited forests. *PLoS ONE* **8**: e69917.
- De Frenne P, Rodriguez-Sanchez F, Coomes DA, *et al.* 2013. Microclimate moderates plant responses to macroclimate warming. *P Natl Acad Sci USA* **110**: 18561–65.
- Dobrowski SZ. 2011. A climatic basis for microrefugia: the influence of terrain on climate. *Glob Change Biol* **17**: 1022–35.
- Duque A, Stevenson PR, and Feeley KJ. 2015. Thermophilization of adult and juvenile tree communities in the northern tropical Andes. *P Natl Acad Sci USA* **112**: 10744–49.
- Engler R, Randin CF, Vittoz P, *et al.* 2009. Predicting future distributions of mountain plants under climate change: does dispersal capacity matter? *Ecography* **21**: 24–45.
- Ettinger AK and HilleRisLambers J. 2013. Climate isn't everything: competitive interactions and variation by life stage will also affect range shifts in a warming world. *Am J Bot* **100**: 1344–55.
- Figge F. 2004. Bio-folio: applying portfolio theory to biodiversity. *Biodivers Conserv* **13**: 827–49.
- Flint LE and Flint AL. 2012. Downscaling future climate scenarios to fine scales for hydrologic and ecological modeling and analysis. *Ecol Processes* **1**: art2.
- Flint LE, Flint AL, Mendoza J, *et al.* 2018. Characterizing drought in California: new drought indices and scenario-testing in support of resource management. *Ecol Processes* **7**: art1.
- Flint LE, Flint AL, Thorne JH, and Boynton R. 2013. Fine-scale hydrologic modeling for regional landscape applications: the California Basin Characterization Model development and performance. *Ecol Processes* **2**: art25.
- Franklin J, Davis FW, Ikegami M, *et al.* 2013. Modeling plant species distributions under future climates: how fine scale do climate projections need to be? *Glob Change Biol* **19**: 473–83.
- Gollan JR, Ramp D, and Ashcroft MB. 2014. Assessing the distribution and protection status of two types of cool environment to facilitate their conservation under climate change. *Conserv Biol* **28**: 456–66.
- Guisan A, Edwards TC, and Hastie T. 2002. Generalized linear and generalized additive models in studies of species distributions: setting the scene. *Ecol Model* **157**: 89–100.
- Hannah L, Flint L, Syphard AD, *et al.* 2014. Fine-grain modeling of species' response to climate change: holdouts, stepping-stones, and microrefugia. *Trends Ecol Evol* **29**: 390–97.
- Hawkins BA, Diniz-Filho AF, Bini LM, *et al.* 2007. Red herrings revisited: spatial autocorrelation and parameter estimation in geographical ecology. *Ecography* **30**: 375–84.
- Holland PG and Steyn DG. 1975. Vegetational responses to latitudinal variations in slope angle and aspect. *J Biogeogr* **2**: 179–83.
- Karger DN, Conrad O, Böhner J, *et al.* 2017. Climatologies at high resolution for the Earth's land surface areas. *Sci Data* **4**: 170122.
- Keppel G, Van Niel KP, Wardell-Johnson GW, *et al.* 2012. Refugia: identifying and understanding safe havens for biodiversity under climate change. *Global Ecol Biogeogr* **21**: 393–404.
- Krawchuk MA, Meigs GW, Cartwright JM, *et al.* 2020. Disturbance refugia within mosaics of forest fire, drought, and insect outbreaks. *Front Ecol Environ* **18**: 235–44.
- Kreft H and Jetz W. 2007. Global patterns and determinants of vascular plant diversity. *P Natl Acad Sci USA* **104**: 5925–30.
- Lawler JJ, Ackerly DD, Albano CM, *et al.* 2015. The theory behind, and the challenges of, conserving nature's stage in a time of rapid change. *Conserv Biol* **29**: 618–29.
- Little EL. 1971. Atlas of United States trees. Volume 1: conifers and important hardwoods. Miscellaneous publication 1146. Washington, DC: US Department of Agriculture, Forest Service.
- Loarie SR, Duffy PB, Hamilton H, *et al.* 2009. The velocity of climate change. *Nature* **462**: 1052–55.
- McCullough IM, Davis FW, Dingman JR, *et al.* 2016. High and dry: high elevations disproportionately exposed to regional climate change in Mediterranean-climate landscapes. *Landscape Ecol* **31**: 1063–75.
- McCune B and Keon D. 2002. Equations for potential annual direct incident radiation and heat load. *J Veg Sci* **13**: 603–06.
- McIntyre PJ, Thorne JH, Dolanc CR, *et al.* 2015. Twentieth-century shifts in forest structure in California: denser forests, smaller trees, and increased dominance of oaks. *P Natl Acad Sci USA* **112**: 1458–63.
- Millar CI and Stephenson NL. 2015. Temperate forest health in an era of emerging megadisturbance. *Science* **333**: 988–93.
- Moeslund JE, Arge L, Bøcher PK, *et al.* 2013. Topography as a driver of local terrestrial vascular plant diversity patterns. *Nord J Bot* **31**: 129–44.
- Morelli TL, Barrows CW, Ramirez AR, *et al.* 2020. Climate-change refugia: biodiversity in the slow lane. *Front Ecol Environ* **18**: 228–34.
- Morelli TL, Maher SP, Lim MCW, *et al.* 2017. Climate change refugia and habitat connectivity promote species persistence. *Climate Change Responses* **4**: 8.
- Oldfather ME, Britton MN, Papper PD, *et al.* 2016. Effects of topoclimatic complexity on the composition of woody plant communities. *AoB Plants* **8**: plw049.

- Paciorek CJ. 2010. The importance of scale for spatial-confounding bias and precision of spatial regression estimators. *Stat Sci* **25**: 107–25.
- Sandel B, Arge L, Dalsgaard B, *et al.* 2011. The influence of Late Quaternary climate-change velocity on species endemism. *Science* **334**: 660–64.
- Segurado P, Araujo MB, and Kunin WE. 2006. Consequences of spatial autocorrelation for niche-based models. *J Appl Ecol* **43**: 433–44.
- Stephenson N. 1990. Climatic control of vegetation distribution: the role of the water balance. *Am Nat* **135**: 649–70.
- Stephenson NL and Das AJ. 2011. Comment on “Changes in climatic water balance drive downhill shifts in plant species’ optimum elevations”. *Science* **334**: 177.
- Suggitt AJ, Wilson RJ, Isaac NJB, *et al.* 2018. Extinction risk from climate change is reduced by microclimatic buffering. *Nat Clim Change* **8**: 713–17.
- Thorne JH, Choe H, Boynton RM, *et al.* 2017. The impact of climate change uncertainty on California’s vegetation and adaptation management. *Ecosphere* **8**: e02021.
- Whittaker RH and Niering WA. 1965. Vegetation of the Santa Catalina Mountains, Arizona: a gradient analysis of the south slope. *Ecology* **46**: 429–52.

This is an open access article under the terms of the Creative Commons Attribution-NonCommercial License, which permits use, distribution and reproduction in any medium, provided the original work is properly cited and is not used for commercial purposes.

■ Supporting Information

Additional, web-only material may be found in the online version of this article at <http://onlinelibrary.wiley.com/doi/10.1002/fee.2204/supinfo>



FrontiersEcoPics

Climbing high to avoid thieves

Each year, during the summer, some coastal areas in southeastern Brazil provide favorable environments for the reproduction of a digger wasp species, the giant *Sphex ingens*. However, the wasps face some hazards. While female wasps bring prey (such as the katydids in these photos) to the nests built on sandy beach soil, some bird species (eg the tropical mockingbird, *Mimus gilvus*) may steal the prey.

Animals that steal food from other animals are called kleptoparasites. This behavior is especially common in birds, and tends to become more frequent in areas with a high concentration of hosts capable of providing abundant, high-quality food. In addition, female wasps carrying prey on the ground are often approached by males for copulation (top photo), creating the opportunity for kleptoparasite attacks. Although females are able to capture and carry prey weighing more than twice their own body mass, it is not uncommon for some females to climb shrubs or trees and launch themselves into flight to reach their nests (bottom photo) instead of dragging prey along the ground.

Observations suggest that there are differences in execution time between wasp prey provisioning behaviors. We hypothesized that climbers would reduce prey exposure time against kleptoparasite attacks by gaining downward flight speed and reducing the occurrence of untimely mating on the ground. However, the question remains: can this behavior also simply be explained by greater energy efficiency in prey transportation?

Carlos Alberto dos S Souza and Jarbas M Queiroz
Federal Rural University of Rio de Janeiro, Seropédica, Brazil
doi:10.1002/fee.2211

